NACA

RESEARCH MEMORANDUM

PERFORMANCE OF A TRANSLATING-DOUBLE-CONE AXISYMMETRIC

INLET WITH COWL BYPASS AT MACH NUMBERS FROM 2.0 TO 3.5

By James F. Connors and George A. Wise

Lewis Flight Propulsion Laboratory Cleveland, Ohio

NATIONAL ADVISORY COMMITTEE FOR AERONAUTICS

WASHINGTON

November 13, 1957 Declassified January 12, 1961

NATIONAL ADVISORY COMMITTEE FOR AERONAUTICS

RESEARCH MEMORANDUM

PERFORMANCE OF A TRANSLATING-DOUBLE-CONE AXISYMMETRIC INLET

WITH COWL BYPASS AT MACH NUMBERS FROM 2.0 TO 3.5

By James F. Connors and George A. Wise

SUMMARY

An experimental investigation to determine the performance characteristics of a translating-double-cone inlet (max. diam. = 16.62 in.) with four variable bypass doors mounted at a forward station on the cowl was conducted in the Lewis 10- by 10-foot unitary wind tunnel at Mach numbers from 2.0 to 3.5. The test Reynolds number based on inlet capture diameter was constant at 3.07×10^6 .

At Mach 3.48, a critical pressure recovery of 0.45 was obtained with a mass-flow ratio of unity and an external drag coefficient of 0.10 based on the maximum frontal area. Over the entire Mach number range, stable reduced-mass-flow operation was achieved by varying the bypass discharge area. The attendant drag rise was far below that for comparable bow-shock spillage and somewhat less than that calculated for spillage behind an oblique shock generated by a 30° half-angle cone. As the bypass doors were opened, moderate decreases in recovery were observed at the higher Mach numbers. Correspondingly, at Mach 2.54 there was no effect, and with detached-shock operation at Mach 1.97 there was even an increase in recovery with increased bypass flow. Effects of angle of attack on internal performance (pressure recovery and exit flow distortion) were typical of axisymmetric inlets.

INTRODUCTION

When a ramjet or turbojet engine is required to operate over a wide Mach number range, matching requirements generally specify that, with fixed-capture-area inlets, large amounts of excess air must be diverted from the engine at off-design Mach numbers. There are three principal methods of handling such excess air: (1) spilling behind a bow shock at the cowl lip, (2) spilling behind an oblique shock, or (3) putting the air through some type of bypass system. Investigation at speeds around Mach 2.0 with a 25° half-angle cone (ref. 1) has shown that a low-angle-discharge bypass has a distinct advantage, drag-wise, over the other two

methods of spilling. This advantage probably persists at speeds above a Mach number of 2.0; however, little experimental data exist on inlet-bypass combinations at these higher speeds.

The present study evaluates a specific inlet-bypass configuration designed to operate at Mach numbers up to 3.5. The inlet was a $25^{\circ}-35^{\circ}$ double-cone translating-spike inlet, and the bypass consisted of four variable doors, 90° apart, located at a forward station on the cowl. At all Mach numbers, the second oblique shock was positioned at the cowl lip. Internal and external performance was determined for various bypass door openings, and a comparison was made between the bypass drag and the drag incurred by spilling behind either an oblique or a bow shock.

The test was conducted in the 10- by 10-foot supersonic wind tunnel at Mach numbers of 3.48, 3.01, 2.54, and 1.97, at angles of attack to 12° , and at a Reynolds number of 2.5×10^{6} per foot.

SYMBOLS

A	area
Ai	inlet capture area, 1.13 sq ft
Amax	maximum projected frontal area of model, 1.507 sq ft
$\mathbf{A}_{\mathbf{X}}$.	area normal to the flow direction in the duct
A ₃	area at diffuser exit (sta. 66.0), 0.961 sq ft
c_{D}	drag coefficient, $\frac{D}{q_0 A_{max}}$
C _{D,c}	cowl pressure drag coefficient, $\frac{1}{r_{\text{max}}^2} \int_{r_{\text{lip}}}^{r_{\text{max}}} c_p dr^2$
^C D,e	external drag coefficient
^C D,e ^C p	static-pressure coefficient, $\frac{p - p_0}{q_0}$
D	drag, 1b
М	Mach number
m_3/m_0	mass-flow ratio, $\frac{\rho_3 V_3 A_3}{\rho_0 V_0 A_1}$

P	total pressure, lb/sq ft
\overline{P}_3	area-weighted average total pressure at station 3, lb/sq ft
\bar{P}_3/P_0	total-pressure recovery
$\frac{P_{3,\text{max}} - P_{3,\text{min}}}{\overline{P}_{3}}$	distortion parameter
p p	static pressure, lb/sq ft
q	dynamic pressure, lb/sq ft
r	radial distance from axis of symmetry, in.
v	velocity, ft/sec
x	axial distance, in.
Y	annular distance across duct, in.
У	radial distance out from centerbody, in.
α	angle of attack, deg
$\theta_{\mathbf{c}}$	spike half-angle, deg
θ_{l}	cowl-lip parameter; i.e., the angle between the axis of symmetry and a line from the spike tip to the cowl lip
ρ	density of air, lb/cu ft
Subscripts:	
max	maximum
min	minimum
0	free-stream conditions
3	conditions at diffuser exit, model station 66 in. from cowl lip

APPARATUS AND PROCEDURE

A schematic drawing of the model is presented in figure 1(a), and photographs of the inlet and bypass-door arrangement are presented in figure 1(b). The model was sting-mounted in the tunnel through a three-component strain-gage balance. In order to vary the inlet back pressure, a movable exit plug was mounted on the sting, independent of the model. Besides the exit plug, the positions of the bypass doors and the spike were varied by remote control.

The inlet was a translating-double-cone inlet designed so that the oblique shocks coalesced at the cowl lip at a Mach number of 3.5. At lower Mach numbers, the spike was translated to maintain the second oblique shock on the lip. The cone half-angles were 25° and 35°, and the initial external cowl lip angle was 23°. Bypassing was accomplished by means of four doors located at a forward station on the cowl (figs. 1(a) and (b)). Each door subtended approximately 25° of the cowl arc and could be rotated about a hinge 4.43 inches aft of the cowl lip. Coordinates for the centerbody, cowl, and bypass doors are given in tables I, II, and III, respectively.

Internal area distributions at the design cowl-lip parameter for each Mach number are presented in figure 1(c). With the spike in the Mach 3.01 position, the over-all diffusion rate was about that of an equivalent 5° conical area expansion. The maximum rate of area expansion occurred between 19 and 22 inches from the cowl lip, where the expansion was equivalent to that of about a 30° cone.

Instrumentation was included in the model to determine pressure recovery, mass-flow ratio, external drag, and cowl pressure drag. Computation of these parameters was performed in the following manner:

- (1) Total-pressure recovery at the diffuser exit (station 3) was based on the area-weighted average of pressures measured by 48 tubes on six radial rakes. An additional tube was placed on each rake to define the flow profile near the sting surface.
- (2) Mass-flow ratio was determined from an average of eight static pressures at station 66 and the assumption of isentropic flow from station 66 to a measured sonic discharge area at station 100. A flow coefficient was determined from a calibration inlet which captured a known free-stream tube of air.
- (3) Total external drag was obtained by subtracting the internal thrust (total momentum change from free stream to exit) from the axial force measured by the strain-gage balance. The base forces were determined by means of static-pressure orifices on the base areas. These forces were not included in the total external drag.

NACA RM E57HO7b

(4) Cowl pressure drags were determined by an investigation of the measured static-pressure distribution on the cowl.

An additional total-pressure rake was installed in the annulus at the cowl lip. The entrance flow was surveyed along a line from the cowl lip perpendicular to the second cone surface.

The investigation was conducted in the 10- by 10-foot supersonic wind tunnel at Mach numbers of 3.48, 3.01, 2.54, and 1.97 and at angles of attack to 12° . The Reynolds number of the test was 2.5×10^{6} per foot.

RESULTS AND DISCUSSION

The internal and external performances of the inlet and bypass combination are presented in figure 2 for the four Mach numbers investigated. At Mach 3.48, the inlet total-pressure recovery at critical was 0.45 with the bypass full closed and the spike at a θ_1 of 32.82°. The corresponding mass-flow ratio was unity with an external drag coefficient of 0.10 based on the maximum frontal area of the inlet. A mass-flow ratio of 0.94 was obtained by extending the spike to a θ_1 of 32.42°. The total-pressure recovery at this condition was essentially the same as at the design condition, but the drag coefficient was markedly increased from 0.10 to 0.145 because of the increased spillage. All data presented in these figures represent stable operating conditions. For each door setting, the last point on the left indicates the minimum stable condition, just prior to the onset of buzz.

With the bypass doors in an open position, the pressure-recovery curves of figure 2 generally show a definite shift in engine mass-flow ratio, while the inlet forward of the bypass station was still operating in the supercritical region. These shifts or steps in the pressure recovery against mass-flow-ratio curves were caused by the terminal shock passing over the bypass doors. As this shock passed across the doors, the pressure ratio between the internal stream and the free stream increased markedly, and the bypass mass flow increased correspondingly.

A cross plot (fig. 3) summarizes the critical inlet performance at zero angle of attack for the range of bypass settings and Mach numbers studied. At Mach 3.48 and 3.01, moderate decreases occurred in total-pressure recovery with increasing bypass mass flows. At $M_{\rm O}=2.54$, the pressure recovery was relatively insensitive to changes in bypass door position. At the $M_{\rm O}=1.97$ condition where a bow shock stood ahead of the cowl lip, the pressure recovery increased with increasing bypass mass flow. This increasing recovery at $M_{\rm O}=1.97$ was the result of the bypass relieving the internal choking in the duct and thereby allowing the terminal shock to be located nearer to the cowl lip.

NACA RM E57HO7b

The upper portion of figure 3 shows the total external drag coefficient at approximately the critical operating condition. Along with these critical values are shown the drag rise due to bow-shock spillage (as determined experimentally during subcritical operation of the inlet) and also the calculated drag rise due to spillage behind an oblique shock generated by a 30° half-angle cone (ref. 2). At Mach 2.54 and above, flow spillage through this bypass system resulted in less drag rise than spillage behind the reference ($\theta_{\rm C}=30^{\rm O}$) oblique shock and much less than spillage behind a bow shock. On the other hand, translation of the 25°-35° double-cone spike would result in a drag rise somewhat intermediate between bow-shock and ($\theta_c = 30^{\circ}$) oblique-shock spillage. This is indicated by the dotted line through the two points, corresponding to Mach 3.48 and the full-closed door position. Typically, the experimental curves of external drag against mass-flow ratio show increasingly steeper slopes with increased bypass mass flow or, correspondingly, with increased door opening. This is, of course, the result of the increased door drag, as it presents a progressively greater angle to the free stream and also to the "cosine" effect on bypass-flow momentum as it discharges at higher and higher angles. For Mach numbers of 2.0 to 3.5, a bypass technique has thus been demonstrated to provide stable inlet operation over a wide range of mass-flow ratios and Mach numbers with no or moderate decrease in recovery and with small associated spillage drags. Such a technique appears quite feasible from an engine-inlet matching viewpoint.

The static-pressure distribution along the external cowl surface at a Mach number of 3.48 and a mass-flow ratio of unity is presented in figure 4. The distribution computed on the basis of two-dimensional shock-expansion theory is also included. Agreement between the two distributions is reasonably good, and the integrated drag coefficients agree within 2 percent. This cowl drag coefficient ($C_{D,C}=0.083$) plus a friction drag coefficient (computed from the von Kármán skin friction coefficient for a turbulent boundary layer) agreed well with the total external drag coefficient derived from the balance and internal pressure measurements.

Radial flow surveys taken at the inlet and exit stations at zero angle of attack for near-critical operation are presented in figure 5. The local total pressures measured near the centerbody were considerably higher than theoretical, particularly at the higher Mach numbers. This additional compression was probably obtained through an extra oblique shock generated by a separation of the spike boundary layer which, in turn, was caused by pressure feedback from the terminal-shock system. A similar flow was observed in the series of tests reported in reference 3. In that investigation, a higher diffuser-exit recovery was obtained through removal of the separated low-energy air with a throat boundary-layer bleed. The similarity of inlet total-pressure profiles here would indicate that the use of a throat bleed in the present case would likewise be promising.

NACA RM E57HO7b

Schlieren photographs that illustrate the supercritical inlet flow patterns at zero angle of attack are presented in figure 6. The first photograph indicates the unity mass-flow-ratio condition at Mach 3.48, while the remaining photographs show the spike at design θ_l for the other Mach numbers. Patterns of the bypass discharge flow are also shown for various door openings.

The angle-of-attack performance of the inlet at near-critical operation and design θ_l is shown in figure 7. The usual decrease in pressure recovery and mass-flow ratio occurred in addition to an increase in external drag coefficient with increasing angle of attack. Opening the bypass doors changed the absolute level of these parameters but had little, if any, effect on their rate of change with angle of attack.

Variation of diffuser-exit flow distortion with angle of attack is presented in figure 8 for near-critical inlet operation. For comparison, the data for the 20° -35° double-cone inlet of reference 4 are also included in the figure. Although the distortion value does increase with angle of attack, the level remains relatively low. Also, opening the bypass doors apparently improves the distortion level over the angle of attack range at $M_{\odot}=3.48$. This improvement does not occur at $M_{\odot}=3.01$ except at zero angle of attack.

SUMMARY OF RESULTS

An axisymmetric translating-double-cone inlet (max. diam. = 16.62 in.) with four variable bypass doors mounted at a forward station on the cowl was evaluated in the Lewis 10- by 10-foot unitary wind tunnel over a Mach number range from 2.0 to 3.5. The following results were obtained:

- 1. At a Mach number of 3.48, a critical pressure recovery of 0.45 was realized with a mass-flow ratio of unity and an external drag coefficient of 0.10 based on the maximum frontal area of the inlet.
- 2. At all Mach numbers, a wide range of stable reduced-mass-flow operation was achieved by varying the exit area of the low-angle sonic-discharge bypass. The attendant drag rise was far below that for comparable spillage behind a bow shock and somewhat less than that calculated for spillage behind an oblique shock generated by a 30° half-angle cone. As the bypass doors were opened, moderate decreases in recovery were observed at the higher Mach numbers. Correspondingly, at the lower Mach numbers, recovery was maintained and, in some cases, increased with increased bypass mass flow.

3. Effects of angle of attack on internal performance (pressure recovery and exit flow distortion) were generally typical of axisymmetric inlets.

Lewis Flight Propulsion Laboratory
National Advisory Committee for Aeronautics
Cleveland, Ohio, August 12, 1957

REFERENCES

- 1. Allen, J. L., and Beke, Andrew: Performance Comparison at Supersonic Speeds of Inlets Spilling Excess Flow by Means of Bow Shock, Conical Shock, or Bypass. NACA RM E53Hll, 1953.
- 2. Sibulkin, Merwin: Theoretical and Experimental Investigation of Additive Drag. NACA Rep. 1187, 1954. (Supersedes NACA RM E51813.)
- 3. Connors, James F., Lovell, J. Calvin, and Wise, George A.: Effects of Internal-Area Distribution, Spike Translation, and Throat Boundary-Layer Control on Performance of a Double-Cone Axisymmetric Inlet at Mach Numbers from 3.0 to 2.0. NACA RM E57F03, 1957.
- 4. Connors, James F., Wise, George A., and Lovell, J. Calvin: Investigation of Translating-Double-Cone Axisymmetric Inlets with Cowl Projected Areas 40 and 20 Percent of Maximum at Mach Numbers from 3.0 to 2.0. NACA RM E57CO6, 1957.

TABLE I. - CENTERBODY COORDINATES

[All dimensions in inches.]

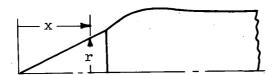
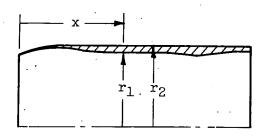


TABLE II. - COWL COORDINATES

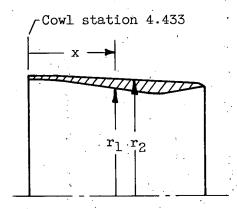
[All dimensions in inches.]



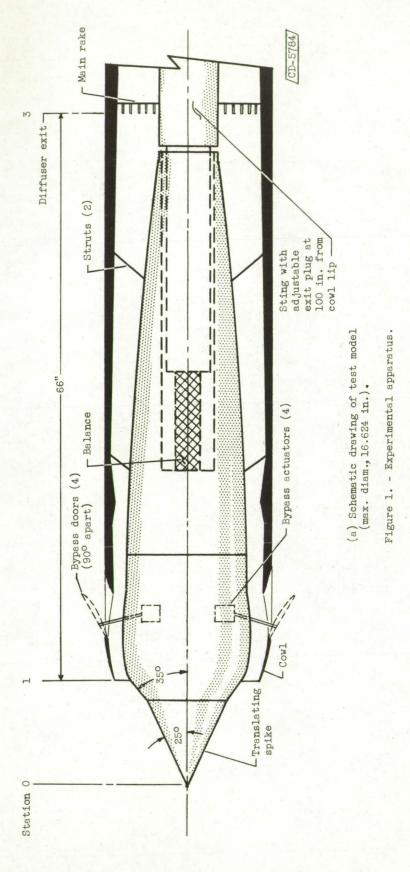
х	rl	r ₂
0 .554 1.108 1.662 2.217 2.770 3.325 3.878 4.433 4.987 5.540 6.095 6.649 7.203 7.757 8.312 8.865 9.365 9.365 9.918 15.820 18.285 21.056 22.500 24.000	7.197 7.425 7.602 7.763 7.907 8.023 8.111 8.156 8.156 8.156 8.134 8.062 7.979 7.896 7.802 7.729 7.646 7.563 7.563 7.563 7.563 7.563 7.563 7.347 7.840 7.840 7.840	7.242 7.481 7.691 7.879 8.040 8.172 8.273 8.312

TABLE III. - BYPASS DOOR COORDINATES (CLOSED POSITION)

[All dimensions in inches.]



х	\mathbf{r}_1	r ₂
0	8.156	8.312
.073	8.156	8.312
.627	8.134	8.294
1.180	8.062	8.273
1.735	7.979	8.239
2:289	7.896	8.239
2.843	7.802	8.239
3.397	7.729	8.239
3.952	7.646	8.239 Cone
4.505	7.591	8.239
5.005	7.563	8.239
5.558	7.563)	8.239
7.165	7.563 Cone	7.868 (Poding
7.290	7.800	7.868 Radius





Three-quarter front view



Front view



(b) Photographs of inlet configuration.

Figure 1. - Continued. Experimental apparatus.

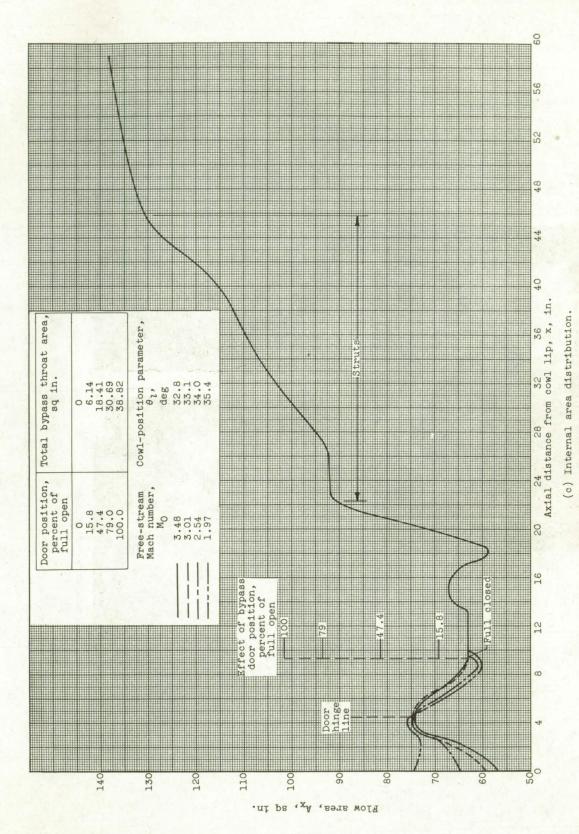


Figure 1. - Concluded. Experimental apparatus.

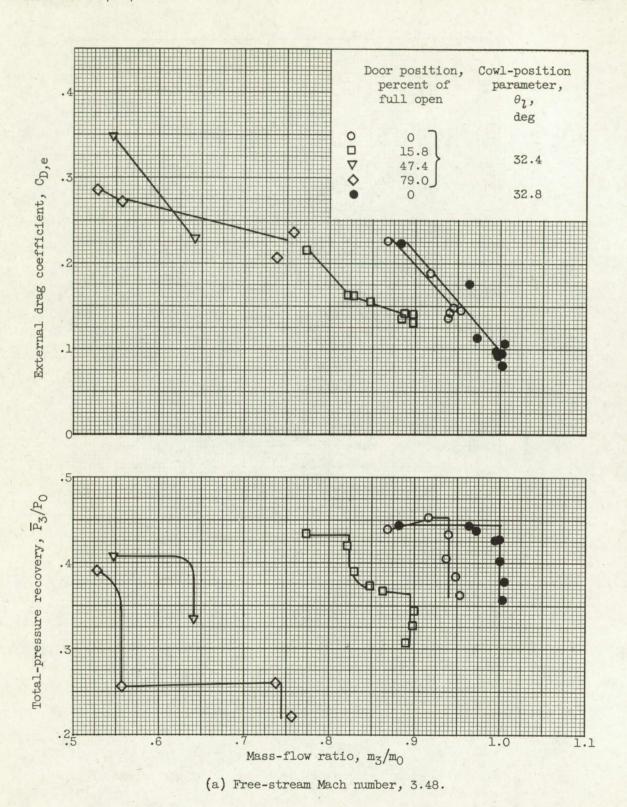
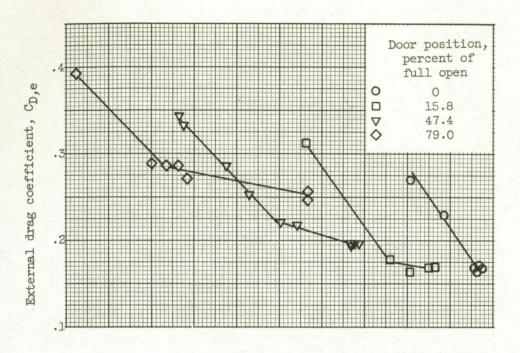
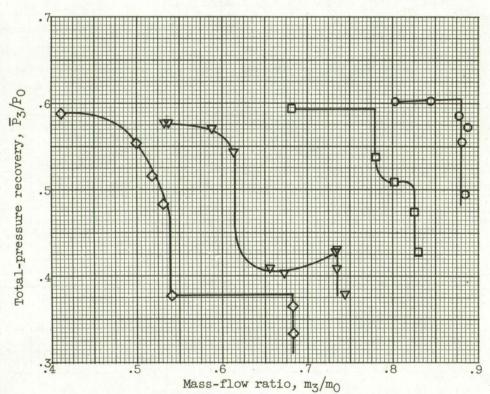


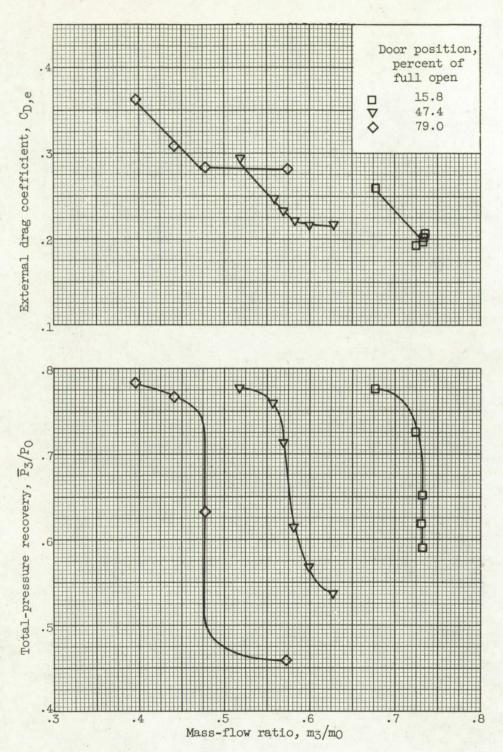
Figure 2. - Performance characteristics at zero angle of attack.





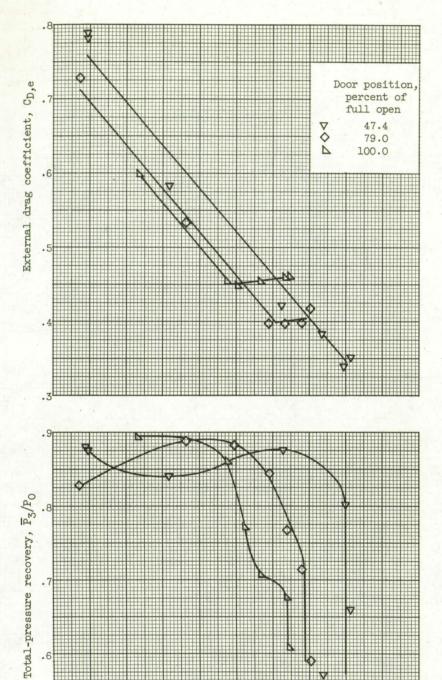
(b) Free-stream Mach number, 3.01; cowl-position parameter, 33.1°.

Figure 2. - Continued. Performance characteristics at zero angle of attack.



(c) Free-stream Mach number, 2.54; cowl-position parameter, 34.0°.

Figure 2. - Continued. Performance characteristics at zero angle of attack.



(d) Free-stream Mach number, 1.97; cowl-position parameter, 35.4° .

Mass-flow ratio, m3/m0

Figure 2. - Concluded. Performance characteristics at zero angle of attack.

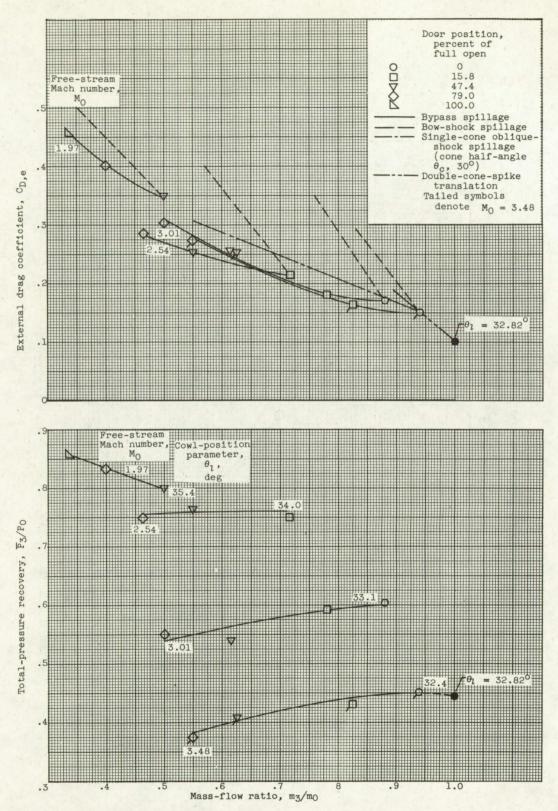


Figure 3. - Critical performance at zero angle of attack for range of Mach numbers.

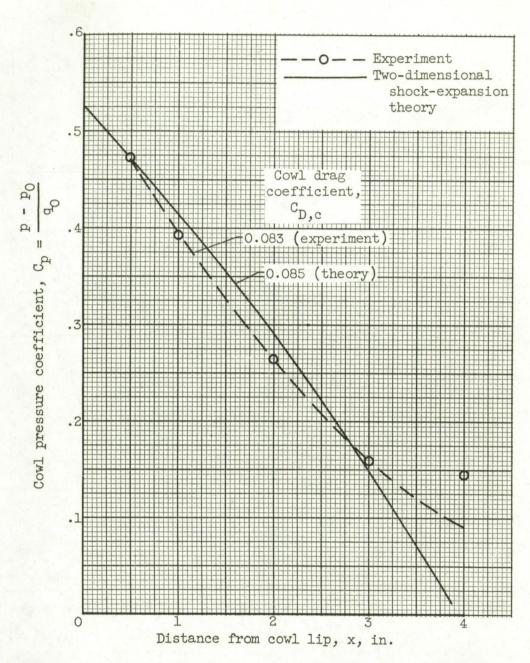
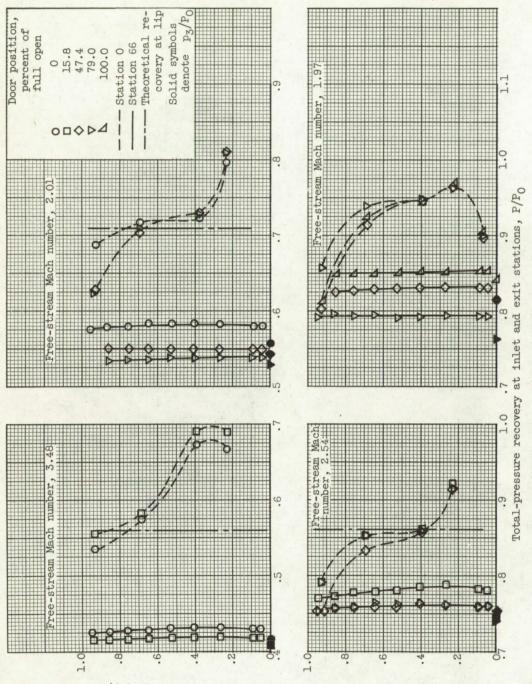


Figure 4. - Static-pressure distribution along cowl. Free-stream Mach number, 3.48; unity mass-flow ratio.

of

Figure 5. - Near-critical total-pressure recovery profiles at inlet and exit stations at zero angle

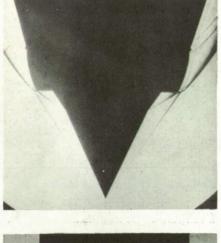
attack and design cowl-position parameter.



Ratio of radial distance from centerbody to duct height, y/Y



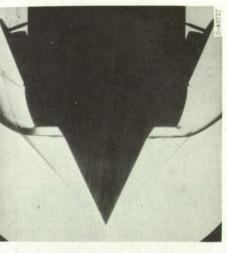
Free-stream Mach number, 3.01; 33.15°; bypass 79 percent of cowl-position parameter, full open

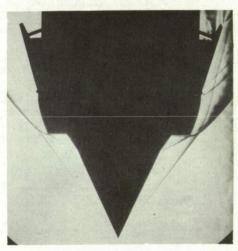


Free-stream Mach number, 3.01; cowl-position parameter, 33.15°; bypass full closed

Free-stream Mach number, 3.48;

cowl-position parameter, 32.82°; bypass full closed





Free-stream Mach number, 2.54; cowl-position parameter, 34.020; bypass 79 percent of full open

Figure 6. - Typical inlet airflow patterns at zero angle of attack.

Free-stream Mach number, 1.97; cowl-position parameter, 35.42°; bypass full open

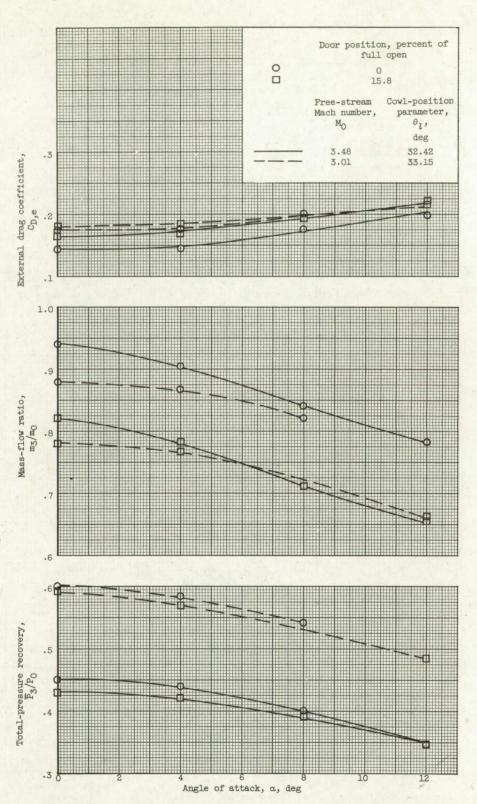


Figure 7. - Effect of angle of attack on performance at approximately critical inlet operation.

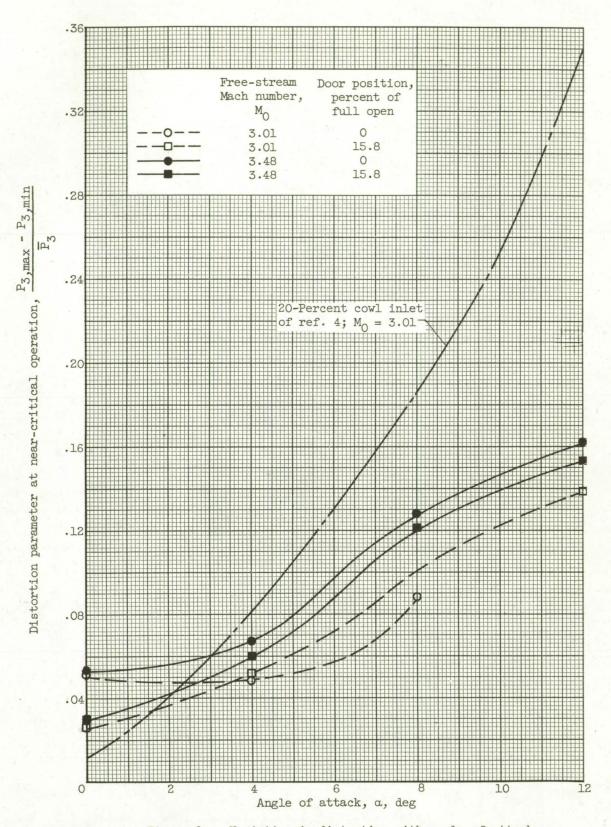


Figure 8. - Variation in distortion with angle of attack.

NOTES: (1) Reynolds number is based on the diameter of a circle with the same area as that of the capture area of the inlet.

(2) The symbol * denotes the occurrence of buzz.

	Description			Test parameters			Test data				Performance			
Report and facility	Configuration	Number of oblique shocks	Type of boundary- layer control	Free- stream Mach number	Reynolds number × 10 ⁻⁶	Angle of attack, deg	Angle of yaw, deg	Drag	Inlet- flow profile	Discharge- flow profile	Flow picture	Maximum total- pressure recovery	Mass-flow ratio	Remarks
RM ES7HO7b Lewis 10- by 10-foot unitary wind tunnel	Four variable bypass doors 350 Translating-double-cone axisymmetric inlet with cowl bypass	2	None	3.48 3.01 2.54 1.97	3.07 3.07 3.07 3.07 3.07	0 to 12	0	V V V	***	**************************************	***	0.45 .60 .76 .86	1.00 to 0.53 .88 to .41 .73 to .39 .50 to .13	At Mach 3.48 the drag coefficient was 0.10 based on maximum frontal area with bypass closed. With bypass spillage, the attendant drag rise was less than bow-shock and oblique-shock (30° half-angle cone) spillage.
RM E57HO7b Lewis 10- by 10-foot unitary wind tunnel	Four variable bypass doors 1 350 Translating-double-cone axisymmetric inlet with cowl bypass	2	None	3.48 3.01 2.54 1.97	3.07 3.07 3.07 3.07	0 to 12	0	777	***	***	***	0.45 .60 .76 .86	1.00 to 0.53 .88 to .41 .73 to .39 .50 to .13	At Mach 3.48 the drag coefficient was 0.10 based on maximum frontal area with bypass closed. With bypass spillage, the attendant drag rise was less than bow-shock and oblique-shock (30° half-angle cone) spillage.
RM E57H07b Lewis 10- by 10-foot unitary wind tunnel	Four variable bypass doors 750 Translating-double-cone axisymmetric inlet with cowl bypass	2	None	3.48 3.01 2.54 1.97	3.07 3.07 3.07 3.07	0 to 12	0	777	***	***	****	0.45 .60 .76 .86	1.00 to 0.53 .88 to .41 .73 to .39 .50 to .13	At Mach 3.48 the drag coefficient was 0.10 based on maximum frontal area with bypass closed. With bypass spillage, the attendant drag rise was less than bow-shock and oblique-shock (30° half-angle cone) spillage.
RM E57H07b Lewis 10- by 10-foot unitary wind tunnel	Four variable bypass doors 350 Translating-double-cone axisymmetric inlet with cowl bypass	2	None	3.48 3.01 2.54 1.97	3.07 3.07 3.07 3.07	0 to 12	0	***	***	****	* * * *	0.45 .60 .76 .86	1.00 to 0.53 .88 to .41 .73 to .39 .50 to .13	At Mach 3.48 the drag coefficient was 0.10 based on maximum frontal area with bypass closed. With bypass spillage, the attendant drag rise was less than bow-shock and oblique-shock (30° half-angle cone) spillage.